Reply to the second reviewer

Thank you for carefully reading the manuscript. We appreciate your informative and insightful comments. Below, we provided an itemized response to all the comments raised, with the original comments presented in blue. Please also see the revised manuscript and the difference file diff.html, which we will submit separately. All the changes made to the manuscript are detailed in diff.html.

Major Comments

2-1) I was quite confused when reading section 2 from 2.1 to 2.7, because I did not understand how you can ensure mass conservation with this set of prognostic attributes. It only became clear when I read section 2.8 and understood that there are no partially melted wet ice particles (yet) in the model. I would strongly recommend to move that statement from section 2.8 to section 2.1 that particles are either liquid (and fully described by radius r) or ice (and described by major and minor axes *a* and *c* and the density ϱ_i).

Following your suggestion, we moved the paragraph from Sec. 2.8 to Sec. 2.1 with some modifications.

> (P. 5, ll. 24-29)
> In this study, for simplicity, partially frozen/melted particles are not considered. We assume that each particle completely freezes or melts instantaneously (see Secs. 4.1.4 and 4.1.5). Therefore, either the equivalent droplet radius r or ice particle attributes $\{a, c, \rho^{\mathrm{i}}\}$ are always zero in our model. Furthermore, we assume that all particles contain soluble substances and are always deliquescent even when the humidity is low (see Sec. 4.1.6). Further, as a crude representation of ``pre-activation'', we do not allow the complete sublimation of an ice particle (see Sec. 4.1.7). Therefore, r and $\{a, c, \rho^{\mathrm{i}}\}$ cannot be simultaneously zero.

2-2) From Figure 8 and 19 I would conclude that snow (aggregates) is falling too fast in SCALE-SDM, i.e. the green data point to not coincide with the empirical relations for aggregates. Can you explain this bias in the fallspeed of snow? I think this should be discussed in the paper.

The bias can be explained by the air density dependence of fall speed. In Figs. 8 and 19, the green slopes for snow aggregates represent the formulas of Locatelli and Hobbs (1974) (LH74 in short) and Heymsfield et al. (2002) (H02 in short). LH74's formulas are for data measured between altitudes of 750 and 1500 m above sea level, hence the density is approximately 1.1 kg m^{-3}. H02's formula is for temperature and pressure of -10 °C and 500 hPa, hence the density is approximately 0.66 kg m^{-3}. In our simulation, most of the snow aggregates exist in the anvil cloud, where the density is approximately 0.38 kg m^{-3}. Khvorostyanov and Curry (2002) estimated that the terminal velocities of large ice particles scale with the ambient density to the power of -1/2. Figure R2-1 below was created by incorporating this density dependence to Fig. 19. That is, we multiplied the LH74's formulas for aggregates by a factor of $(0.38\,\mathrm{kgm^{-3}}/1.1\,\mathrm{kgm^{-3}})^{-1/2} \approx 1.70$, and the formula of H02 for aggregates by a factor of $(0.38\,\mathrm{kgm^{-3}}/0.66\,\mathrm{kgm^{-3}})^{-1/2} \approx 1.32$. Now the agreement between our model results and the formulas is much better.

To clarify this point, the above discussion is added to Sec. 7.3 "Ice particle morphology and fall speeds"

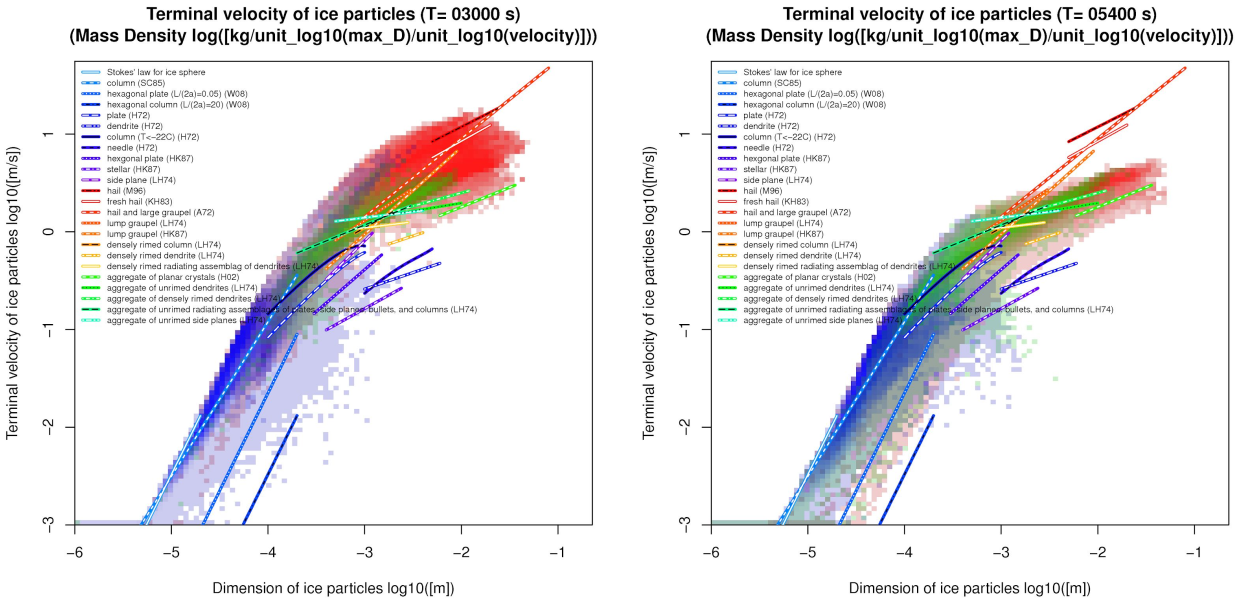

Figure R2-1. Same as Fig. 19 but with snow aggregates formulas (green slopes) adjusted to an air density of 0.38 kg m^{-3}.

2-3) Maybe related to that: Wouldn't it be more accurate to use an ellipse instead of the circumcircle for the area in Boehms formula (section 4.1.3, page 11, line 20)? Do you take into account the turbulence correction for large Reynolds numbers in Boehms equations? The latter is actually necessary to limit the fall speed of large aggregates and match the observed terminal fall speed of aggregates.

As explained in our reply to Comment 2-2, the fall speeds of snow aggregates in our model compare well with other formulas if the air density difference is considered. Regarding the turbulence correction, yes, it is incorporated in our model (see Eq. R2-1 below). However, we learned that circumscribed ellipse instead of circumcircle has to be used in Böhm's formula. We also learned that the characteristic length in Böhm's formula is not given by the maximum dimension. Nevertheless, based on the assessment presented below, we confirmed that these corrections do not change the behavior of the cloud significantly, and hence, this flaw causes only a minor impact on this study.

Noting that area ratio $q_i \leq 1$ always holds in our model, Böhm (1989,1992,1999)'s formula $v^{\infty}_{\text{Böhm}}(m_i, \phi_i, d_i, q_i; \rho_i, T_i)$ can be summarized as follows:

$$X = \frac{8 m_i g \rho}{\pi \mu^2 \max(\phi_i, 1) q_i^{1/4}},$$

$$X' = X \frac{1 + (X/X_0)^2}{1 + 1.6 (X/X_0)^2}, \qquad \text{R2-1}$$

$$X_0 = 2.8 \times 10^6, \quad \text{for ice particles},$$

$$k = \min\left\{ \max(0.82 + 0.18\phi_i, 0.85), \left(0.37 + \frac{0.63}{\sqrt{\phi_i}}\right), \frac{1.33}{\max(\log\phi_i, 0) + 1.19} \right\},$$

$$\Gamma = \max\{1, \min(1.98, 3.76 - 8.41\phi_i + 9.18\phi_i^2 - 3.53\phi_i^3)\},$$

$$C_{\mathrm{DP}} = \max(0.292k\Gamma, 0.492 - 0.200/\sqrt{\phi_i}),$$

$$C_{\mathrm{DO}} = 4.5k^2 \max(\phi_i, 1),$$

$$\beta = \left[1 + \frac{C_{\mathrm{DP}}}{6k}\left(\frac{X'}{C_{\mathrm{DP}}}\right)^{1/2}\right]^{1/2} - 1,$$

$$\gamma = \frac{C_{\mathrm{DO}} - C_{\mathrm{DP}}}{4C_{\mathrm{DP}}},$$

$$N_{\mathrm{Re}} = \frac{6k}{C_{\mathrm{DP}}}\beta^2\left[1 + \frac{2\beta e^{-\beta\gamma}}{(2+\beta)(1+\beta)}\right],$$

$$v^{\infty}_{\mathrm{Böhm}} = \frac{\mu N_{\mathrm{Re}}}{\rho d_i}.$$

In SCALE-SDM 0.2.5-2.2.0/2.2.1, we assumed that the characteristic length d_i is given by the maximum dimension $D_i = 2\max(a_i, c_i)$, and area ratio q_i is given by the the area ratio with respect to the circumcircle $q_i^{\mathrm{cc}} = A_i/A_i^{\mathrm{cc}}$, but we learned this is not correct. In Böhm's theory, they are defined by

$$d_i = 2a_i, \quad q_i = q_i^{\mathrm{ce}} = A_i/A_i^{\mathrm{ce}}, \qquad \text{R2-2}$$

i.e., for columnar particles, minor axis is used for the characteristic length d_i, and the area ratio with respect to the circumscribed ellipse is used for q_i. Figure 1 in Böhm (1989) suggests $q_i = q_i^{\mathrm{ce}}$. It is not clearly specified, but from the second equality of Eq. 17 in Böhm (1992), we can confirm that $d_i = 2a_i$.

For planar ice particles ($\phi_i < 1$), $v^{\infty}_{\mathrm{Böhm}}(d_i = 2a_i, q_i = q_i^{\mathrm{ce}})$ and $v^{\infty}_{\mathrm{Böhm}}(d_i = D_i, q_i = q_i^{\mathrm{cc}})$ yield the same results, because $2a_i = D_i$ and $q_i^{\mathrm{ce}} = q_i^{\mathrm{cc}}$ hold for $\phi_i < 1$. However, for columnar ice particles ($\phi_i > 1$), $v^{\infty}_{\mathrm{Böhm}}(D_i, q_i^{\mathrm{cc}})$ always underestimates the fall velocity. From the above equations, we can derive $v^{\infty}_{\mathrm{Böhm}}(2a_i, q_i^{\mathrm{ce}})/v^{\infty}_{\mathrm{Böhm}}(D_i, q_i^{\mathrm{cc}}) = \phi_i^{3/4}$ for $X \ll 1$, and $v^{\infty}_{\mathrm{Böhm}}(2a_i, q_i^{\mathrm{ce}})/v^{\infty}_{\mathrm{Böhm}}(D_i, q_i^{\mathrm{cc}}) = \phi_i^{7/8}$ for $X \gg 1$. Therefore, if $\phi_i = 2$, the ratio $v^{\infty}_{\mathrm{Böhm}}(2a_i, q_i^{\mathrm{ce}})/v^{\infty}_{\mathrm{Böhm}}(D_i, q_i^{\mathrm{cc}})$ is in the rage of 1.68–1.83; if $\phi_i = 10$, the range is 5.62–7.50; if $\phi_i = 20$, it is 9.46–13.75. From Fig. R2-2 we can confirm that Böhm's original definition $v^{\infty}_{\mathrm{Böhm}}(2a_i, q_i^{\mathrm{ce}})$ agrees well with the formulas of Westbrook (2008), and Heymsfield and Westbrook (2010).

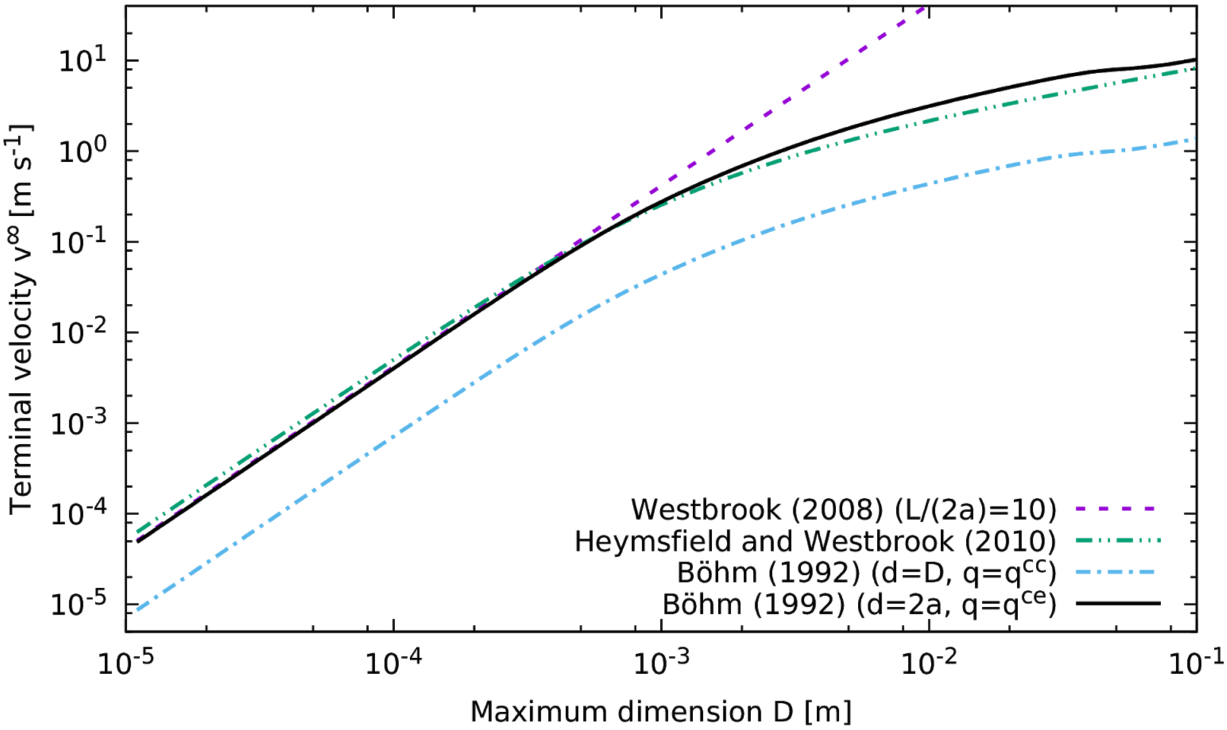

Figure R2-2. Comparison of terminal velocity formulas for long ice particles with aspect ratio $\phi = 10$. Westbrook (2008)'s formula is applicable only to small ice particles. Böhm (1992)'s formula with the correct d and q agrees well with other formulas.

Therefore, the correction R2-2 generally increases the fall speed of columnar ice particles, and the increase factor is larger for longer particles. Then, through the ventilation effects (13) and (17), the diffusional growth of columnar ice particles is enhanced. Due to this mechanism, we observed a creation of very long ice particles with aspect ratio $\phi > 100$ if we incorporate the correction R2-2 to SCALE-SDM 0.2.5-2.2.1. However, this is unrealistic. The maximum aspect ratio reported is approximately 30 in Auer and Veal (1970) (see Fig. 12 therein), and 15.77 in Um et al. (2015). In nature, such an extreme shape ice particle would be shattered spontaneously or by collision, but for the moment, we fix this issue in an ad-hoc way; we do not allow an ice particle to grow by diffusion slenderer than $\phi = 40$ by imposing a limiter to the effective inherent growth ratio Γ^* as follows.

$$\Gamma^* = 1 \quad \text{for } dm_i \geq 0 \ \wedge \ \phi_i > 40. \qquad \text{R2-3}$$

We incorporated the corrections R2-2 and R2-3 into SCALE-SDM 0.2.5-2.2.1 to create a revision, SCALE-SDM 0.2.5-2.2.2. To assess the impact of these corrections, we conducted the same simulation as the typical realization of CTRL using the new model. We observed that the precipitation was developed a few minutes faster, but the total precipitation amount was almost the same as the previous versions (Fig. R2-3). Figure R2-4 compares the time evolution of water paths. Here, a noticeable decrease of graupel water path can be observed, which is attributed to the faster fall speed of columnar graupel particles (i.e., densely rimed columns). This in turn increased the rain water path. The time evolution of other hydrometeor water paths (cloud, cloud ice, and snow) were almost unchanged. Ice particle morphology distributions resemble closely to the previous results except the vanishment of cloud ice particles with relatively slow terminal velocities (Figs. R2-5 -- R2-8. See also Movies 13--16 in the Supplement). The corrections do not alter the spatial structure of the cloud either (Movie 12 in the Supplement).

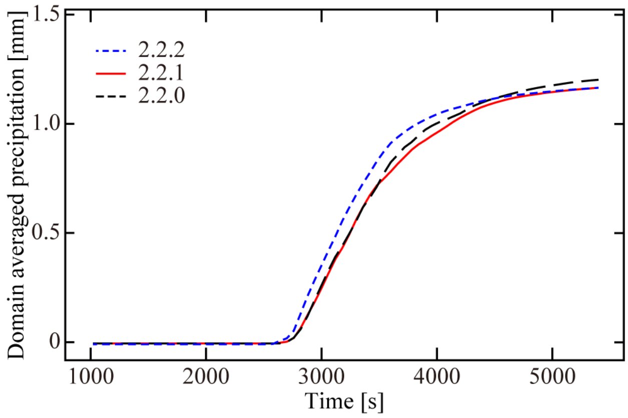

Figure R2-3. Changes in accumulated precipitation amounts before and after corrections. The long dashed, solid, and short dashed lines represent the SCALE-SDM 0.2.5-2.2.0, -2.2.1, and -2.2.2, respectively.

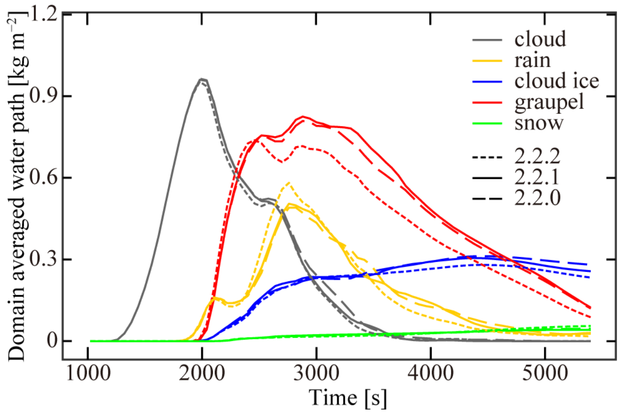

Figure R2-4. Changes in the domain-averaged water path before and after corrections. The long dashed, solid, and short dashed lines represent the SCALE-SDM 0.2.5-2.2.0, -2.2.1, and -2.2.2, respectively.

Based on the above discussion, we have made various revisions to the manuscript. Major changes are summarized as follows.

Title of the manuscript is slightly modified:
old< Predicting the morphology of ice particles in deep convection using the super-droplet method: development and evaluation of SCALE-SDM 0.2.5-2.2.0/2.2.1
----
new> Predicting the morphology of ice particles in deep convection using the super-droplet method: development and evaluation of SCALE-SDM 0.2.5-2.2.0, -2.2.1, and -2.2.2

In Sec. 4.1.3 “Ice particle terminal velocity”, the second paragraph is added to inform the readers that $d_i = 2a_i$ and $q_i = q_i^{\mathrm{ce}}$ are the correct definition.

In Figs. 20 and 21, the results of SCALE-SDM 0.2.5-2.2.2 are now included.

Section 9.2 “Fix of ice particle terminal velocity implementation” is added. Here, the impact of the corrections $d_i = 2a_i$ and $q_i = q_i^{\mathrm{ce}}$ on this study is assessed in detail.

SCALE-SDM 0.2.5-2.2.2 is released on the software repository.

List of symbols is updated.

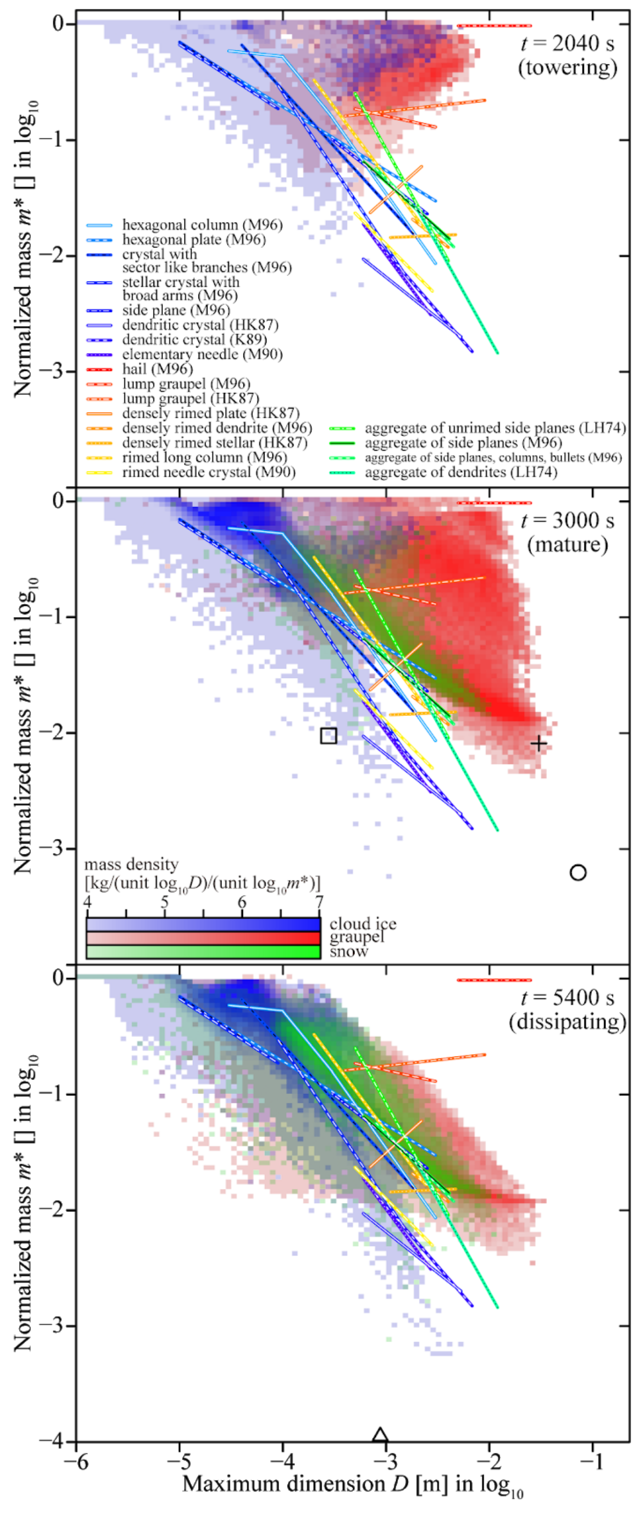

Figure R2-5. Same as Fig. 5 but shows results from SCALE-SDM 0.2.5-2.2.2. See also Movie 13 in the Supplement.

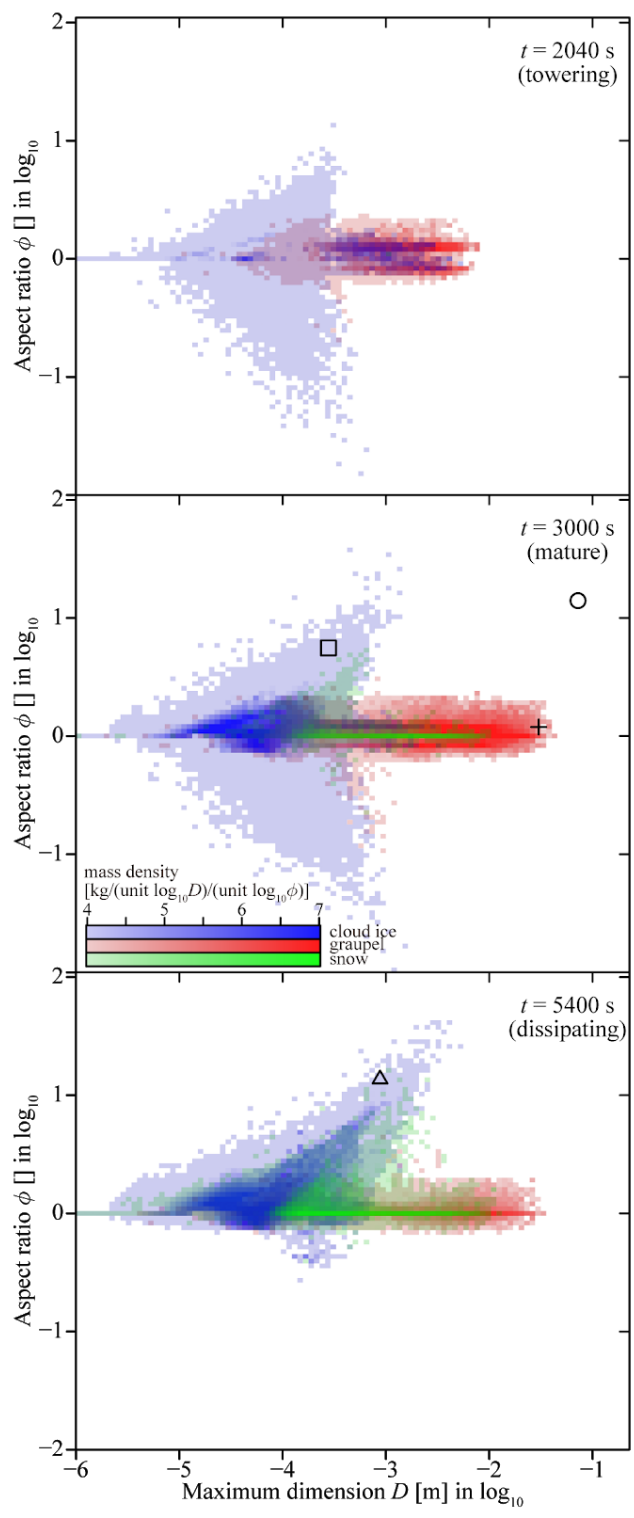

Figure R2-6. Same as Fig. 6 but shows results from SCALE-SDM 0.2.5-2.2.2. See also Movie 14 in the Supplement.

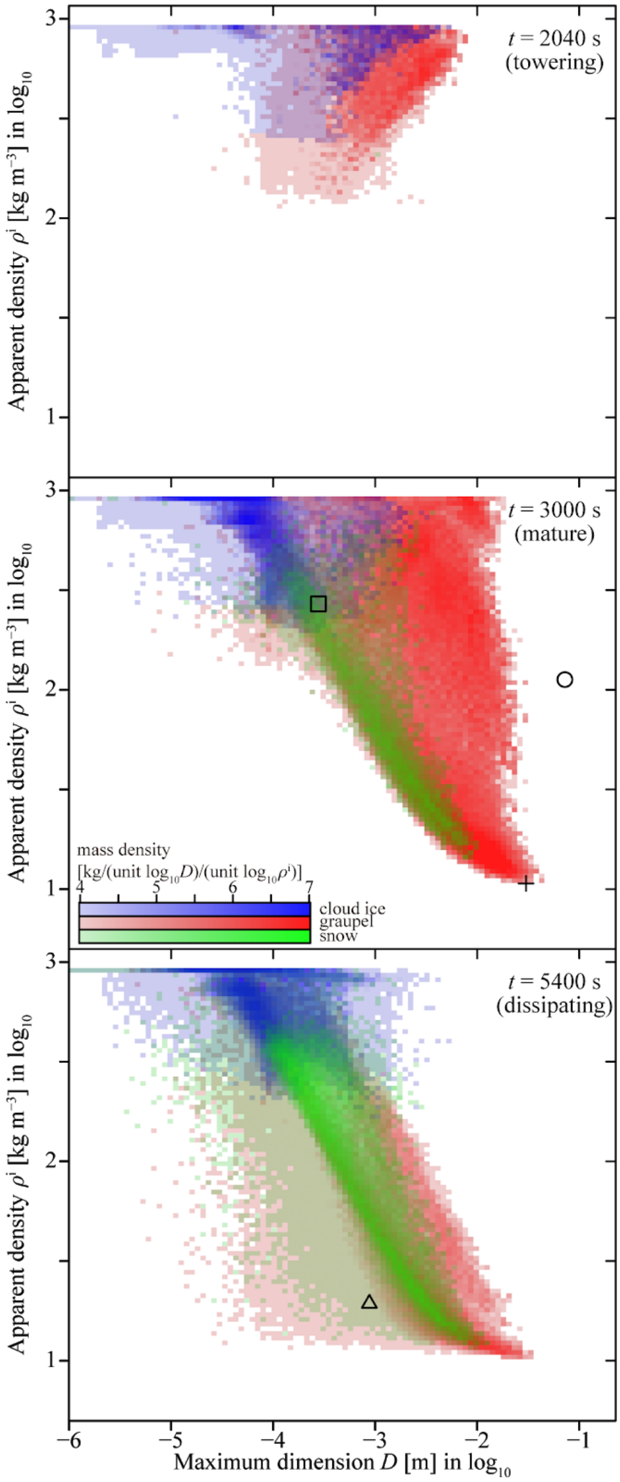

Figure R2-7. Same as Fig. 7 but shows results from SCALE-SDM 0.2.5-2.2.2. See also Movie 15 in the Supplement.

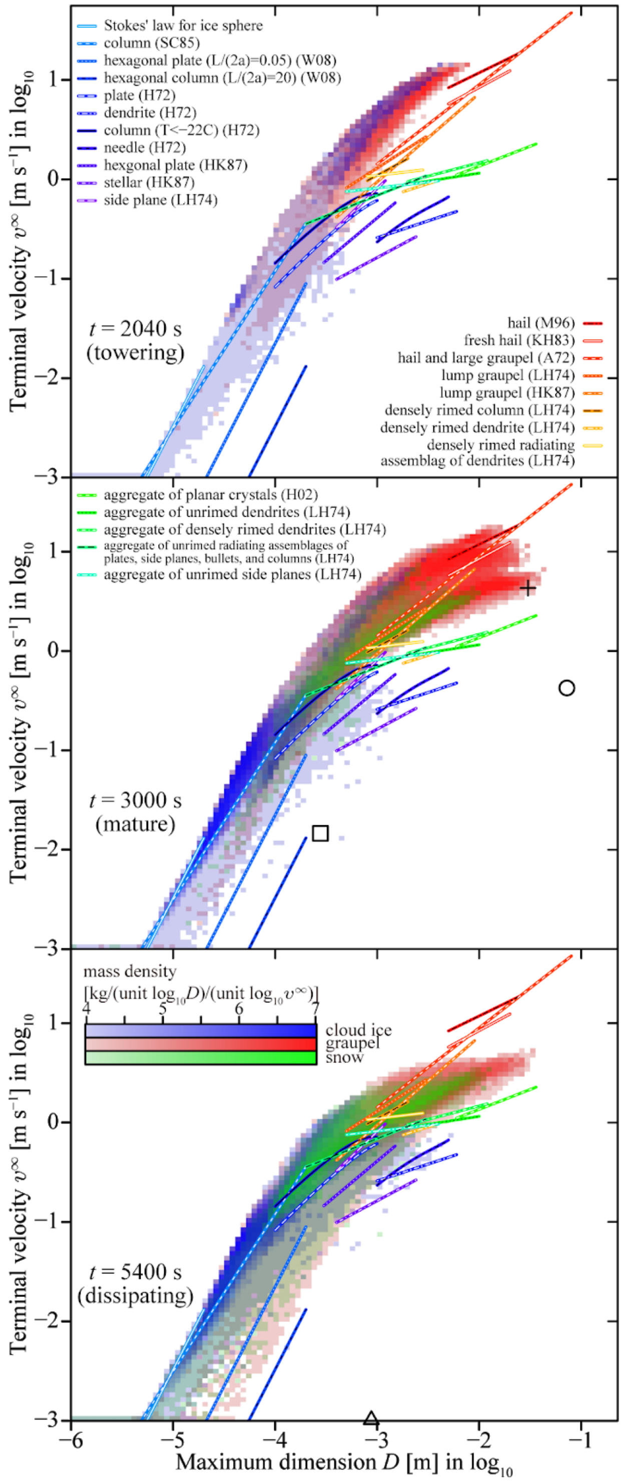

Figure R2-8. Same as Fig. 8 but shows results from SCALE-SDM 0.2.5-2.2.2. See also Movie 16 in the Supplement.

Minor Comments

2-4) page 5, line 5-7: I agree that a rigorous theory for bulk models is still lacking, but it would nevertheless be appropriate to reference the review by Beheng (2010). This paper gives an overview of the steps that have been made towards such a theoretical foundation, at least for liquid clouds and rain.

To clarify our argument, we have rephrased the part as follows.

(P. 2, ll. 14-21)
old< … They solve a mathematical model that is closed in lower moments of the distribution function of cloud droplets, rain droplets, and ice particle categories (e.g., total mass and total number of particles). Currently, bulk models do not have a rigorous theoretical foundation and must rely on empirical parameterizations. A more bottom-up approach to construct more accurate and reliable numerical models would thus be desired.

new> … They solve a mathematical model that is closed in the lower moments of the distribution function of cloud droplets, rain droplets, and ice particle categories (e.g., mass and number mixing ratios). The basic premise of bulk models is that the distribution function can be determined by the lower moments, but such a universal relationship is unknown. In other words, in bulk models, to predict the time evolution of a chosen set of moments, their time derivatives are approximated by some functions of the moments being predicted, but this is not generally possible (see, e.g., Beheng, 2010). It would be also informative to note the analogy and difference between the Navier--Stokes equation and bulk models (Morrison et al., 2020), which highlights the difficulty in deriving bulk models. Therefore, for cloud microphysics, a more bottom-up approach to construct more accurate and reliable numerical models would be desired.

2-5) page 6, line 4: ’approximated by a histogram’, here I would recommend to replace ’histogram’ by ’finite volumes or finite differences’.

We agree that ‘histogram’ would be awkward as an explanation of a numerical scheme, but it has an affinity to ’bin’. Therefore, we rephrased the sentence as follows.

(P. 3, ll. 19-21)
old< Bin schemes adopt an Eulerian approach and the particle distribution function is approximated by a histogram.

new> Bin schemes adopt an Eulerian approach and the particle distribution function is approximated using a finite number of control volumes (histogram).

2-6) page 5, line 8: ’breakdown of the Smoluchowski equation’. Not all readers might be familiar with the notion of the breakdown of the Smoluchowski equation. A reference other than Smoluchowski (1916) or an additional sentence would be helpful.

We have added Alfonso and Raga (2017), and Dziekan and Pawlowska (2017).

2-7) page 9, section 2.7: It should be mentioned that the assumption that particles move at their terminal fall velocity is an approximation. In the framework of a Lagrangian particle model this can quite easily be improved by considering the adjustment towards the new terminal fall velocity, e.g., after a collision event (see e.g. Naumann and Seifert 2015).

We clarified that it is a simplification. Sec. 2.7 “Velocity” is modified as follows.

(P. 7, l. 18)
old< We consider that each particle is always moving at its terminal velocity.

new> We approximate that each particle is always moving at its terminal velocity.

New paragraph is added to Sec. 4.1.1 “Advection and sedimentation”

(P. 8, ll. 25-27)
In this study, we assume that terminal velocity is always achieved instantaneously; however,

this is a simplification. The relaxation time of large droplets is a few seconds (Fig. 3 of Wang and Pruppacher (1977)). The acceleration of particles can be considered by explicitly solving the motion equation (see, e.g., Naumann and Seifert (2015)).

2-8) page 13, section 4.1.6: When I first read this paragraph I was surprised that the ventilation is missing and is not even mentioned. It would be good to mention this approximation already here and not only later in section 9.2.4.

We have added the following explanation to the paragraph.

(P. 11, ll. 15-18)
The growth of a droplet by condensation/evaporation is governed by Eqs. (8)-(10) in our model. When a droplet or an ice particle falls through the air, the flow around it enhances the diffusional growth, a phenomenon known as the ventilation effect. It does not essentially affect the growth of droplets smaller than $50\,\mu m$ in radius (see Sec. 13.2.3 of Pruppacher and Klett (1997)). Therefore, for simplicity, we do not consider the ventilation effect on droplets in this study. ...

2-9) page 14, eq. (13): Why is the minimum mass m^i_{min} necessary in this equation? Is this because homogeneously frozen droplets may not contain any insoluble aerosol mass and then you would eventually have a super-droplet with zero mass? Does that m^i_{min}-particle not grow immediately when it is advected into cold, ice-supersaturated conditions and produce unrealistic ice? It does remember its freezing temperature, but it is already ice and would therefore grow immediately when the environment is supersaturated with respect to ice. I don't understand how this is implemented.

This is a crude expression of pre-activation. Next to Eq.(14) we have added the following explanation.

(P. 12, ll. 18-21)
This is a crude representation of pre-activation (see, e.g., Marcolli, 2017, for a review). Each particle keeps the memory of ice activation until the ambient temperature rises above $0\,^\circ\mathrm{C}$; A particle with $m^{\mathrm{i}}_{\mathrm{min}}$ ice grows immediately after the ambient air is supersaturated over ice irrespective of its freezing temperature T_i^{fz}.

We have also added the following discussion to Sec. 9.3.1 "Ice nucleation pathways"

(P. 61, ll. 28-34)
A crude model of pre-activation is incorporated in our model by inhibiting complete sublimation (see Eq. (14) and the explanation follows). Pre-activation denotes ``the capability of particles or materials to nucleate ice at lower relative humidities or higher temperatures compared to their intrinsic ice nucleation efficiency after having experienced an ice nucleation event or low temperature before'' (Marcolli, 2017). Intensive sophistication based on laboratory studies is required; however, particle-based models are suitable for exploring the atmospheric relevance of pre-activation. Conversely, one might want to switch off pre-activation in our model, which is possible by resetting the particles as deliquescent aerosol particles when complete sublimation occurs.

2-10) page 15, eq. (21): Why is it necessary to impose this explicit limit to water saturation? If water droplets are present, then the supersaturation should be limited to due the rapid condensational growth. If no water droplets are present and no CCN can be activated, then the limit to water saturation might be unphysical.

First of all, note that the limit to water saturation only applies to the deposition density formula of Chen and Lamb (1994a) given in Eq. (20). It is not clarified in Chen and Lamb (1994a), but Miller and Young (1979) suggested to use the same deposition density at and above water saturation. Maybe they assumed this simply because no data was available above water saturation, but in order to avoid the use of an unrealistically low deposition density, we followed their suggestion.

2-11) page 15 and 16: For depositional growth it is assumed that particle are spherical for *D* smaller than 10 microns (top of page 15), but for sublimation it is assumed that particles become spherical only when smaller than 1 micron. Why this asymmetry/hysteresis?

In SCALE-SDM 0.2.5-2.2.0, $\Gamma(T)=1$ for $D<10\,\mu m$ applies to both deposition and sublimation. In SCALE-SDM 0.2.5-2.2.1 and -2.2.2, $\Gamma=1$ is always assumed for sublimation. $\Gamma=1$ just preserves the aspect ratio during sublimation/deposition (if ventilation effect is ignored), hence the creation of very small planar or columnar ice particles can happen, which occurs particularly when they sublimate. Therefore, we decided to reset the shape of an ice particle as spherical when it is very small. Radius of minor axis smaller than $1\,\mu m$ is the criteria we introduced. We have to admit this is not based on a rigorous physical consideration, but it would be justified because $1\,\mu m$ is roughly the boundary between the continuum and kinetic regimes. The specific value of the criteria would not be very important; we can expect that almost all submicron sized, sublimating ice particles will sublimate completely almost instantaneously. Still, it is worth mentioning that the spherical resetting we introduced is beneficial for numerical simulation; if $\phi_i=1$, Eq. (11) without the ventilation effect reduces to a simple form $dm_i^{2/3}/dt=\mathrm{const.}$

2-12) page 16, line 14: 'rime mass fraction does not change during sublimation'. According to equation (29) rime mass fraction does not change during deposition (dm > 0) and only change during sublimation (dm < 0). Do you mean 'rime mass fraction does only change during sublimation'.

The definition of rime mass fraction is $m_{\mathrm{i}}^{\mathrm{rime}}/m_{\mathrm{i}}$, hence both the text and the equation are correct. To avoid confusion, we have clarified the definition of rime mass fraction.

2-13) page 17, line 16: 'remove k from the system'. Do you remove the particle because you have not yet introduced the multiplicity in those equations? Isn't it confusing to give here a Monte-Carlo algorithm without multiplicity, which is (as I assume) not used in SCALE-SDM. Maybe it should be emphasized (again) that this is the underlying theoretical model, but not the numerical implementation.

To clarify and emphasize that the section is devoted to the description of the underlying theoretical model, we have added the following paragraph at the end of the subsection.

> (End of Sec. 4.1.9 "Coalescence between two droplets")
> Let us emphasize that the stochastic model introduced in this section describes the underlying mathematical model of coalescence process, not the Monte Carlo algorithm of SDM that solves the stochastic process numerically. In the preceding paragraph, droplet k was removed from the system because both j and k are real particles. On the contrary, in the SDM, the number of super-particles is (almost always) conserved through coalescence (Shima et al., 2009).

2-14) page 21, line 16: Why c_j+min(a_k, c_k)? Shouldn't it be c_j+max(a_k, c_k) for the longest possible minor axis?

Even when a pair of ice particles stick together and construct an aggregate with the maximum possible volume, we still assume that these ice particles are falling with their maximum dimension perpendicular to the flow direction. Probably it rarely happens that planar or columnar ice particles rotate vertically and stick together at a right angle, like the shape of "T".

2-15) page 24, line 4: 'other planets planets'. Two times 'planets'.

We have fixed the typo.

2-16) page 28, section 5.5.5: Would it be possible to discuss the time step of the Monte Carlo scheme in some more detail? Or is this basically the same argument as in Shima et al.(2009) on page 1313?

The time step can be determined from the same argument, but in the revised manuscript we put it in a slightly different way to provide a precise physical interpretation. See the second and third paragraphs of Sec. 5.5.5 “Coalescence, riming, and aggregation”.

2-17) page 27, line 3: ’predictor-collector’, maybe ’predictor-corrector’?

We have fixed the typo.

2-18) page 44, line 11-12: ’Figure 10 clearly indicates that the super-particle number concentration must be larger than 128/cell’. This is not obvious to me. From Figure 10 I would conclude that 64/cell or even 32/cell is actually fine. Can you explain how you determined the value of 128/cell.

We jumped to the conclusion, but we admit it is not obvious. To provide a quantitative basis, we have conducted a statistical hypothesis test, the result of which is summarized in Table R2-1.

The equality of variances and averages are tested by F-test and T-test, respectively. “2-512” indicates that the column corresponds to the test between NSP002 and NSP512. The same applies to other column headers. CWP, …, and SWP represent the maximum water path of each hydrometeor type plotted in Fig. 10. “prec” represents the accumulated precipitation amount plotted in Fig. 9. The number in each cell represents the p-value, i.e., the probability that the actual difference is greater than the observed difference under the null hypothesis that the variances or averages of the two ensembles are equal. Yellow and green indicate that there exists a significant difference with a confidence level of 99% and 95%, respectively. Blue indicates that the equality cannot be rejected.

Our F-test could not detect a significant difference in variances in most of the cases. From the T-test, we confirmed that the numerical convergence of CWP is slow, which can be observed also in Fig. 10. This is closely related to the onset of warm rain through coalescence; From Fig. 10, we can find that the maximum of cloud water path coincides with the emergence of rainwater. Therefore, a small shift of the warm rain onset time changes the maximum value, but it does not have a big impact on the overall properties of the simulated cloud. Indeed, with a few exceptions, the maximum water paths of all the other hydrometeor types do not show a significant difference if super-particle number concentration is larger than 64 or 128/cell.

All in all, we may conclude that numerical convergence with respect to super-particle number is fairly well achieved at 128/cell, but 64/cell would be also acceptable.

Based on the above discussion, we have revised the manuscript as follows.

> (P. 45, ll. 1-11)
> Figure 9 indicates that the accumulated precipitation amount is less sensitive to the super-particle number. However, Fig. 10 reveals that the initial super-particle number concentration c^{SP} affects the maximum water path statistics. The numerical convergence of maximum cloud water path is noticeably slow. This is closely related to the onset of warm rain through coalescence. From Fig. 3, we determine that the maximum of the cloud water path coincides with the emergence of rainwater. Therefore, a small shift of the warm rain onset time changes the maximum cloud water path; however, it does not have a considerable impact on the overall properties of the simulated cloud. The maximum water paths of all the other hydrometeor types do not show a significant difference if c^{SP} is larger than 64 or 128/cell (see also Table R2-1 of authors' response to anonymous referee #2). When the number of super-particles was too low, more rain droplets were produced because of an erroneous enhancement of collision-coalescence that suppressed the amount of cloud droplets, cloud ice particles, and graupel particles.

To summarize, we may conclude that numerical convergence regarding the super-particle number is fairly well achieved at NSP128 (CTRL), i.e., $c^{\mathrm{SP}} = 128/cell$.

F-test (H0: two variances are equal)

	2-512	4-512	8-512	16-512	32-512	64-512	128-512	256-512
CWP	0.0080	0.0690	0.3131	0.7480	0.7210	0.7772	0.5606	0.5758
RWP	0.1061	0.3265	0.3044	0.5608	0.2523	0.3157	0.8333	0.1567
CIWP	0.3214	0.8093	0.7933	0.8478	0.7260	0.2142	0.0446	0.0368
GWP	0.0457	0.1412	0.0502	0.8361	0.5501	0.0034	0.6177	0.0839
SWP	0.0425	0.0157	0.2712	0.6814	0.2791	0.4521	0.7480	0.6340
prec	0.0229	0.3057	0.0145	0.0507	0.0897	0.1556	0.6828	0.2113

F-test (H0: two variances are equal)

	2-256	4-256	8-256	16-256	32-256	64-256	128-256	512-256
CWP	0.0019	0.0205	0.1225	0.8108	0.3620	0.7812	0.2580	0.5758
RWP	0.8313	0.6512	0.6852	0.3932	0.7764	0.6675	0.2242	0.1567
CIWP	0.0034	0.0613	0.0640	0.0553	0.0166	0.3638	0.9285	0.0368
GWP	0.7671	0.7828	0.8007	0.1245	0.2447	0.1702	0.2082	0.0839
SWP	0.1112	0.0456	0.5264	0.3779	0.1243	0.2240	0.4272	0.6340
prec	0.2682	0.8150	0.1955	0.4518	0.6356	0.8581	0.3934	0.2113

T-test (H0: two averages are equal)

	2-512	4-512	8-512	16-512	32-512	64-512	128-512	256-512
CWP	8.E-28	3.E-26	5.E-24	8.E-21	6.E-19	2.E-13	4.E-09	0.0258
RWP	4.E-09	3.E-08	2.E-06	0.0007	0.0370	0.5484	0.7741	0.5956
CIWP	3.E-11	3.E-09	2.E-08	4.E-06	4.E-05	0.0120	0.3656	0.1916
GWP	6.E-12	4.E-10	6.E-09	4.E-05	0.0024	0.0011	0.0623	0.0297
SWP	9.E-09	2.E-07	3.E-08	9.E-08	0.0195	0.6384	0.4855	0.4595
prec	0.1901	0.9715	0.9218	0.1673	0.9969	0.6853	0.2584	0.2232

T-test (H0: two averages are equal)

	2-256	4-256	8-256	16-256	32-256	64-256	128-256	512-256
CWP	3.E-26	1.E-24	1.E-22	1.E-19	2.E-17	9.E-12	3.E-06	0.0258
RWP	8.E-12	2.E-10	1.E-08	2.E-05	0.0017	0.1561	0.3664	0.5956
CIWP	4.E-06	4.E-05	0.0002	0.0151	0.0890	0.4621	0.7240	0.1916
GWP	7.E-14	3.E-11	6.E-10	0.0004	0.0725	0.0422	0.9301	0.0297
SWP	7.E-09	1.E-07	2.E-08	9.E-08	0.0057	0.2244	0.1683	0.4595
prec	0.9852	0.1224	0.0858	0.0013	0.0929	0.2658	0.9686	0.2232

Table R2-1. F-test and T-test for statistically testing the equality of variances and averages, respectively. “2-512” indicates that the column corresponds to the test between NSP002 and NSP512. The same applies to other column headers. CWP, …, and SWP represent the maximum water path of each hydrometeor type plotted in Fig. 10. “prec” represents the accumulated precipitation amount plotted in Fig. 9. The number in each cell represents the p-value, i.e., the probability that the actual difference is greater than the observed difference under the null hypothesis that the variances or averages of the two ensembles are equal. Yellow and green indicate that there exists a significant difference with a confidence level of 99% and 95%, respectively. Blue indicates that the equality cannot be rejected.

2-19) page 60, line 14: 'approximating the particle is spherical' -> 'as spherical'

We have fixed the typo.

2-20) page 60 and elsewhere: I find collision-riming and collision-aggregation awkward wording. Riming and aggregation are always due to collisions. Hence, the prefix 'collision' is not necessary.

Good idea. Coalescence also always accompanies collision. We removed “collision-” from the manuscript unless otherwise it is misleading.

2-21) page 60, line 25: First sentence of 9.2.7 'We assume that collision-riming's collection efficiency'. Should this read aggregation instead of riming?

We have fixed the typo.

2-22) page 62, line 9: 'Seifert et al. (2005)'s model'. This is actually the Low and List (1982) breakup model combined with Beard and Ochs (1995) for small drops. Seifert et al. (2005) did not add anything new to the physics of the breakup process.

We decided to cite Prat et al. (2012) to introduce breakup models. They tested several combinations of existing models, such as Low and List (1982), Seifert et al. (2005) (compilation of Low and List (1982) and Beard and Ochs (1995)), Testik et al. (2011), and McFarquhar (2004).

2-23) page 62, line 13-15: I would recommend to delete the two sentences starting with 'On average,...'. This is very questionable, has not been shown in the paper and would, in my opinion, be just a compensation of errors. Such a compensating effect is not a good reason to ignore breakup processes.

We have deleted the two sentences. We admit that the thought experiment assessing the impact is too simplified and misleading.

References

Alfonso, L. and Raga, G. B.: The impact of fluctuations and correlations in droplet growth by collision–coalescence revisited – Part 1: Numerical calculation of post-gel droplet size distribution, Atmos. Chem. Phys., 17, 6895–6905, https://doi.org/10.5194/acp-17-6895-2017, 2017.

Auer, A.H. and D.L. Veal, 1970: The Dimension of Ice Crystals in Natural Clouds. J. Atmos. Sci., 27, 919–926, https://doi.org/10.1175/1520-0469(1970)027<0919:TDOICI>2.0.CO;2

Böhm, H.P., 1989: A General Equation for the Terminal Fall Speed of Solid Hydrometeors. J. Atmos. Sci., 46, 2419–2427, https://doi.org/10.1175/1520-0469(1989)046<2419:AGEFTT>2.0.CO;2

Böhm, J. P.: A general hydrodynamic theory for mixed-phase microphysics. Part I: drag and fall speed of hydrometeors, Atmospheric Research, 27, 253–274, https://doi.org/10.1016/0169-8095(92)90035-9, 1992.

Böhm, J. P.: Revision and clarification of 'a general hydrodynamic theory for mixed-phase microphysics', Atmospheric Research, 52, 167–176, https://doi.org/10.1016/S0169-8095(99)00033-2, 1999.

Dziekan, P. and Pawlowska, H.: Stochastic coalescence in Lagrangian cloud microphysics, Atmos. Chem. Phys., 17, 13509–13520, https://doi.org/10.5194/acp-17-13509-2017, 2017.

Heymsfield, A. J., Lewis, S., Bansemer, A., Iaquinta, J., Miloshevich, L. M., Kajikawa, M., Twohy, C., and Poellot, M. R.: A general approach for deriving the properties of cirrus and stratiform ice cloud particles, Journal of the Atmospheric Sciences, 59, 3–29, https://doi.org/10.1175/1520-0469(2002)059<0003:AGAFDT>2.0.CO;2, 2002.

Heymsfield, A.J. and C.D. Westbrook, 2010: Advances in the Estimation of Ice Particle Fall Speeds Using Laboratory and Field Measurements. J. Atmos. Sci., 67, 2469–2482, https://doi.org/10.1175/2010JAS3379.1

Khvorostyanov, V.I. and J.A. Curry, 2002: Terminal Velocities of Droplets and Crystals: Power Laws with Continuous Parameters over the Size Spectrum. J. Atmos. Sci., 59, 1872–1884, https://doi.org/10.1175/1520-0469(2002)059<1872:TVODAC>2.0.CO;2

Locatelli, J. D. and Hobbs, P. V.: Fall speeds and masses of solid precipitation particles, Journal of Geophysical Research, 79, 2185–2197, https://doi.org/10.1029/jc079i015p02185, 1974.

Morrison, H., van Lier-Walqui, M., Fridlind, A. M., Grabowski, W.W., Harrington, J. Y., Hoose, C., Korolev, A., Kumjian, M. R., Milbrandt, J. A., Pawlowsk, H., Posselt, D. J., Prat, O. P., Reimel, K. J., Shima, S.-I., van Diedenhoven, B., and Xue, L.: Confronting the challenge of modeling cloud and precipitation microphysics, under review at Journal of Advances in Modeling Earth Systems, 2020.

Um, J., McFarquhar, G. M., Hong, Y. P., Lee, S.-S., Jung, C. H., Lawson, R. P., and Mo, Q.: Dimensions and aspect ratios of natural ice crystals, Atmos. Chem. Phys., 15, 3933–3956, https://doi.org/10.5194/acp-15-3933-2015, 2015.